Porous fission fragment tracks in fluorapatite

Weixing Li,[1,2,3] Lumin Wang,[1,2,*] Kai Sun,[1] Maik Lang,[3] Christina Trautmann,[4] and Rodney C. Ewing[1,2,3,†]
[1]*Department of Materials Science and Engineering, University of Michigan, Ann Arbor, Michigan 48109-2104, USA*
[2]*Department of Nuclear Engineering and Radiological Sciences, University of Michigan, Ann Arbor, Michigan 48109-2104, USA*
[3]*Department of Geological Sciences, University of Michigan, Ann Arbor, Michigan 48109-1005, USA*
[4]*GSI Helmholtz Centre for Heavy Ion Research, Planckstr. 1, 64291 Darmstadt, Germany*
(Received 17 July 2010; published 18 October 2010)

Fission tracks caused by the spontaneous fission of ^{238}U in minerals, as revealed by chemical etching, are extensively used to determine the age and thermal history of Earth's crust. Details of the structure and annealing of tracks at the atomic scale have remained elusive, as the original track is destroyed during chemical etching. By combining transmission electron microscopy with *in situ* heating, we demonstrate that fission tracks in fluorapatite are actually porous tubes, instead of having an amorphous core, as generally assumed. Direct observation shows thermally induced track fragmentation in fluoapatite, in clear contrast to the amorphous tracks in zircon, which gradually "fade" without fragmentation. Rayleigh instability and the thermal emission of vacancies control the annealing of porous fission tracks in fluorapatite.

DOI: 10.1103/PhysRevB.82.144109 PACS number(s): 61.82.Ms, 61.46.Fg, 68.35.Md, 91.80.Rx

I. INTRODUCTION

In fluorapatite $[Ca_{10}(PO_4)_6F_2]$, which represents 70% of all the fission track age determinations,[1] the track along the trajectory of a fission fragment has been considered to be a cylinder of radiation-damaged amorphous material,[2–4] similar to the tracks in other minerals, such as zircon $(ZrSiO_4)$.[5] The atomic-scale structure of, unetched (often called "latent"), fission tracks controls temperature-induced "fading" and finally leads to shortening of the etchable length of a track.[6,7] Despite the important application to thermochronology, there has been no systematic study of the internal structure of fission tracks and how they evolve on thermal annealing. The present understanding of the process is largely limited to mathematical fits to data on etched track lengths as a function of temperature, time, and composition.[1,7–10] Even a highly cited physical model of the process has met with considerable criticism[9,11,12] in the absence of actual observations of the atomic-scale process. This model[9] is based on the assumption that track annealing in apatite is a process of atom-by-atom recombination within an amorphous track. Here, we report direct observations of the internal structure of tracks and the thermal annealing process of fluorapatite by combining advanced *in situ* transmission electron microscopy (TEM) with thermal treatments at elevated temperatures. We also compare the annealing behavior of apatite to zircon, for which the tracks are amorphous. These TEM observations of *in situ* thermal annealing of fission tracks provide a bridge between the current empirical models of annealing and a fundamental understanding of the atomic-scale process.

II. EXPERIMENTAL

Two types of tracks in fluorapatite were investigated in this study: (1) randomly oriented thermal-neutron-induced tracks from fission of ^{235}U created in the naturally occurring, fluorapatite from Durango, Mexico and (2) parallel tracks produced in the same material by exposing 50 μm thick single crystals to 2.2 GeV Au ions in 5×10^{10} ions/cm^2. Ion irradiations were performed at the UNILAC accelerator of the GSI Helmholtz Centre for Heavy Ion Research (Darmstadt, Germany) under beam incidence parallel to the *c*-axis of the crystals. 2.2 GeV Au ions create tracks of 90 μm length much longer as compared with typical fission fragments (e.g., 100 MeV Xe ions, ~10 μm). The electronic energy loss per unit path length of ions, dE/dx, is determined by the mass and kinetic energy of the projectiles being 16 keV/nm for 100 MeV Xe ions and 26 keV/nm for 2.2 GeV Au ions. However, this difference in energy loss per unit of depth does not result in significant differences in the track morphology.[13] Parallel tracks were also produced in zircon by exposing 50 μm thick single crystals to 2.2 GeV Au ions in 5×10^{10} ions/cm^2. TEM studies were conducted with a JEM 2010F electron microscope. To avoid possible further irradiation-induced damage during sample thinning by ion milling, all TEM samples were crushed and suspended on a carbon film supported by Cu grid. During the TEM observation, the electron current density was kept as low as possible (0.1–1 A/cm^2) to minimize electron-irradiation-induced microstructural changes.

III. RESULTS AND DISCUSSION

A. Atomic structure of tracks in fluorapatite

Details on the damage structure depend on the target material and energy deposition. Tracks in many oxides and complex ceramics are amorphous cylinders embedded within the crystalline matrix.[5,13,14] In polymers, high-energy ion irradiation produces many volatile chemical species resulting in the creation of free volume.[15] Direct TEM observation of tracks in organic materials is difficult, as the structure is modified rapidly under the electron beam.[15] Voidlike structures are also known to develop under ion irradiation in other solids, e.g., CaF_2 and fluorapatite,[16,17] generating volatile decomposition products, but the nature of these apparently porous structures has not been directly confirmed.

Randomly oriented neutron-induced fission tracks within a fluorapatite can be directly observed by TEM when they are slightly out of focus (Fig. 1). The random orientation of

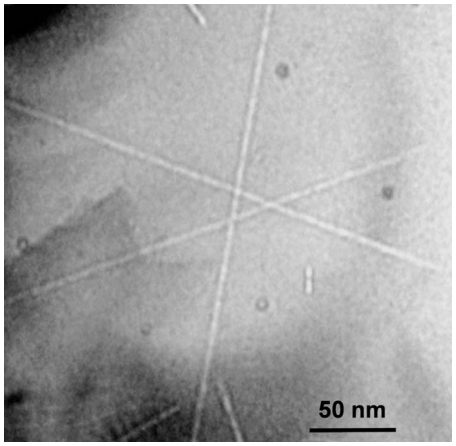

FIG. 1. Randomly oriented neutron-induced fission tracks embedded in fluorapatite as observed by TEM. There are no fundamental differences in the nature of the tracks created by the spontaneous fission of ^{238}U or the neutron-induced fission of ^{235}U.

damage trails requires extended focusing efforts; thus, it is extremely difficult to record high-resolution TEM (HRTEM) images of individual tracks without causing beam-induced modifications to the initial track structure. This problem is avoided by investigating parallel tracks produced by irradiation with swift heavy ions. By adjusting the incidence angle of the ion beam, tracks can be aligned along a specific zone axis for easy HRTEM analysis of tracks in cross section. A low electron current density ($\sim$0.5 A/cm^2) was used to minimize the electron-beam damage. The highly porous tracks produced with 2.2 GeV Au ions in fluorapatite were directly observed by HRTEM (Fig. 2). The central core region of the track has the same bright contrast as the free space outside the sample grain, suggesting that no solid components remain in the track core. This is significantly different from the particle-induced tracks in zircon and other ceramics and minerals, where the amorphous features can be clearly seen in the track core.[5,13,14] In addition, both dark

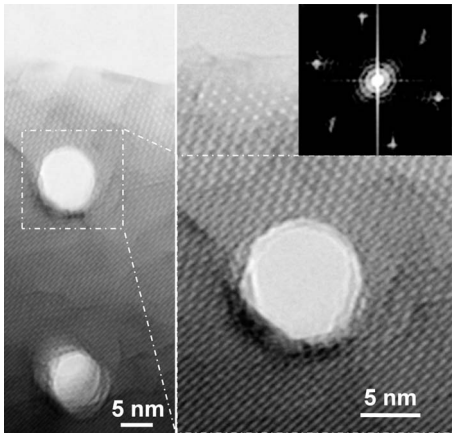

FIG. 2. Plan view HRTEM images of tracks induced by 2.2 GeV Au ions showing a highly porous core. The tracks are deliberately produced along the *c*-axis of a fluorapatite single crystal. Airy pattern shown in the FFT image (inset) is caused by the electron diffraction from the highly porous track, acting as an aperture.

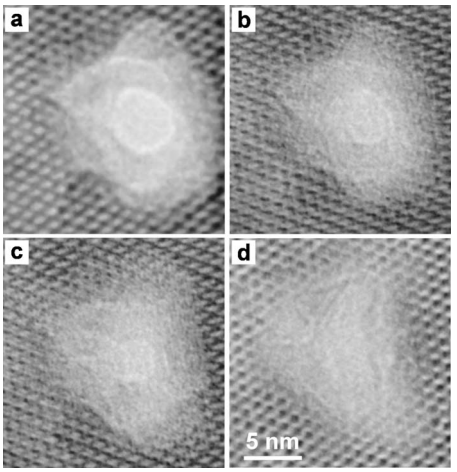

FIG. 3. [(a)–(d)] Plan view HRTEM images with an imaging interval of $\sim$2 min showing exposure to electron beam at room temperature causes the newly formed matter gradually cover the core region of an initially porous track in fluorapatite created by 2.2 GeV Au ion.

rings and hexagonal diffraction spots can be seen in the fast Fourier transform (FFT) image centered on a track in apatite (Fig. 2). The diffraction spots result from the {0001} and $\{1\bar{1}00\}$ planes in the hexagonal structure of fluorapatite. The dark rings are probably the Airy pattern caused by the diffraction from the highly porous track, acting as an aperture. By measuring the radius of each ring (R_i), the diameter of the track (D) can be calculated based on the equation for circular aperture diffraction,

$$\frac{R_i}{L} = 1.22\frac{\lambda}{D},\ 2.23\frac{\lambda}{D},\ 3.24\frac{\lambda}{D}\cdots, \tag{1}$$

where the camera length ($L\lambda$) can be obtained from the diffraction spots. All of the calculated diameters match well with the ones (8–9 nm) observed by HRTEM. The Airy pattern further confirms that the tracks in apatite are highly porous.

We recorded the dynamic process of the change in morphology of tracks in fluorapatite under continuous electron-beam irradiations in order to determine whether exposure to the electron beam during observation can change the initially amorphous tracks into porous channels. However, the electron-beam irradiations ($\sim$0.5 A/cm^2) caused the originally porous track to be gradually filled with new material (Fig. 3). Several measurements were made in order to reduce the radiation damage during sample preparation and observation. As a result, the porous tracks in fluorapatite could be imaged (Fig. 2), rather than the highly damaged tracks (Fig. 3) and as have been reported in other studies.[17]

Further evidence that the latent tracks in fluorapatite are highly porous was obtained by electron energy-loss spectroscopy (EELS) in TEM mode using the Gatan GIF system that allows one to compare the thickness maps of a fission track that penetrates the entire thickness of the sample to holes drilled by a focused electron beam (Fig. 4). As marked in the image [Fig. 4(a)], we deliberately drilled a sequence of five

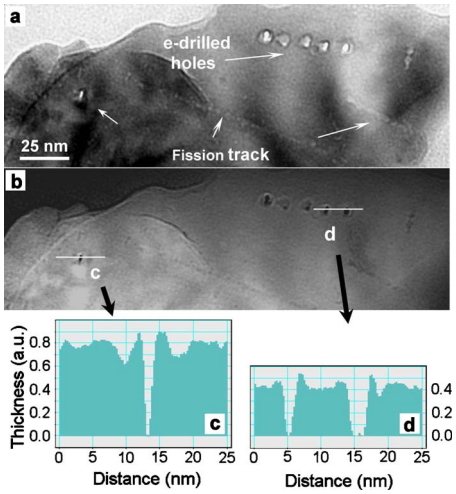

FIG. 4. (Color online) Thickness map. TEM images are obtained from a region where a fission track penetrates through the entire fluorapatite layer. Five small holes in close proximity to the track were deliberately drilled using the focused electron beam. (a) Energy filtered elastic image. (b) Thickness map. (c) Thickness profile along line "c" through the fission track as highlighted in the lower left of (b). (d) Thickness profile along line "d" cutting through two electron-beam-drilled holes as highlighted in the upper right part of image (b).

small holes in close proximity to the track.[18,19] EELS has the advantage that it separates the inelastically scattered electrons and this increases with sample thickness.[20,21] This phenomenon allowed us to directly compare the signal from the fission track and the electron-beam-drilled channel [Fig. 4(b)]. The thickness profiles from the fission track and the two electron-drilled holes are shown in Figs. 4(c) and 4(d), respectively. In the central core, the thickness signal of the fission track is as low as the background of the sample, indicating that the track completely passes through the entire thickness of the sample, similar to that observed for the electron-beam-drilled holes, confirming that the fission track is highly porous.

In situ heating experiments were conducted using a TEM heating stage at 700 °C in order to fill the highly porous tracks in fluorapatite with foreign elements. Zhang and Su[22] have shown that Cu atoms from the TEM copper grid diffuse into carbon nanotubes at 600 °C. The increased mobility of Cu atoms at elevated temperature results in the formation of Cu nanorods inside the nanotubes, as well as the random accumulation of spherical Cu nanoparticles on the carbon film.[22] During the heating of fission tracks, we observed that similar spherical Cu nanoparticles formed immediately at 700 °C and were randomly distributed on the fluorapatite surface and the supporting carbon film on the Cu grid [Fig. 5(b)]. Interestingly, the Cu atoms diffuse through the track opening into some of the highly porous fission tracks, forming cylindrical Cu nanorods [Fig. 5(b)]. The immediately filling of foreign elements into the nanochannel at high temperatures suggests it is through capillary action.[23]

Fresnel contrast techniques were used to compare the internal structure of tracks in fluroapatite to tracks in zircon (Fig. 6). Fresnel contrast techniques with TEM can be used

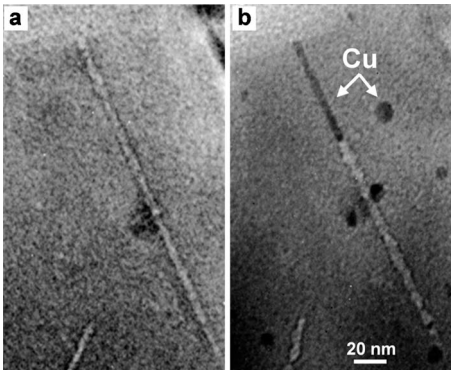

FIG. 5. *In situ* heating of fission tracks in fluorapatite. TEM images (a) before heating and (b) after the temperature stabilizes at 700 °C for 1 min show that, Cu atoms from the supporting copper grid diffuse into a fission track through the open end and form a nanorod inside the track.

to directly observe bubbles or voids in solids.[20] When the image is in focus, a cavity is almost invisible. However, one can obtain maximum contrast around the cavity by a change in focus conditions, i.e., a dark core and bright fringe at the over focus condition and a bright core and dark fringe at the under focus condition. It is the large difference in the inner potential (or density) between the cavity and the surrounding solid that accounts for the contrast change at different focus conditions.[20] Fresnel contrast was obvious around both fission tracks in fluorapatite and 2.2 GeV Au ions induced tracks in fluorapatite [Figs. 6(a) and 6(b)], suggesting a large potential difference between the tracks and the surrounding solid. The release of volatile elements during decomposition has been reported to cause a density deficiency of ~50%

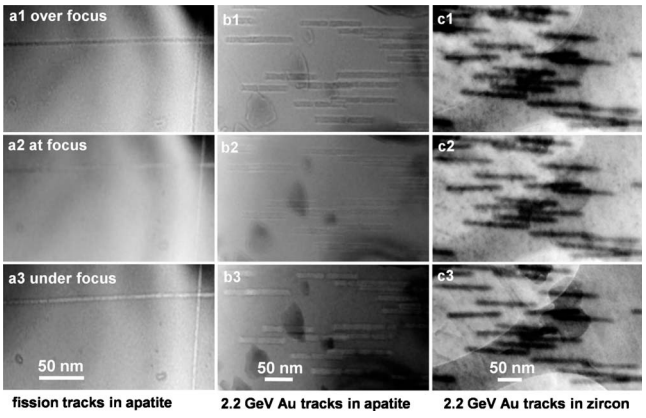

FIG. 6. Fresnel contrast. TEM images of (a) fission tracks in apatite, (b) 2.2 GeV Au ion induced tracks in apatite, and (c) 2.2 GeV Au ion-induced tracks in zircon at (1) over focus, (2) focus, and (3) under focus conditions. Fresnel contrast from fission tracks and swift ion tracks in apatite can be observed by changing focus: (a1) and (b1) over focus image of a track has a dark core surrounded by a bright fringe; (a2) and (b2) at focus image has little phase contrast; and (a3) and (b3) under focus image of a track has a bright core surrounded by a dark fringe. However, no fringe can be observed around the tracks in zircon, and the contrast in the tracks remains constant whenever the focus condition changes from (c1) over focus, (c2) at focus, to (c3) under focus.

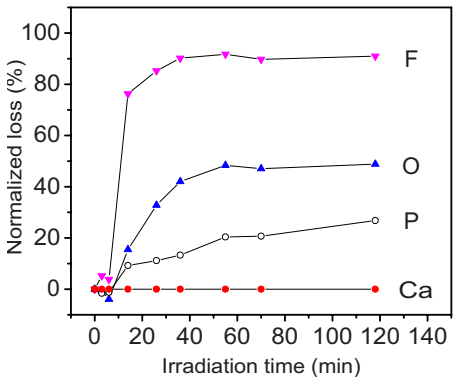

FIG. 7. (Color online) EDS analysis. The loss of different volatile elements normalized to Ca content. The exposure of fluorapatite to 200 keV electrons was performed in a TEM applying a high current (~ 5 A/cm^2) for up to 118 min.

across the 3.2 nm diameter of ion tracks in LiF, as determined by small-angle x-ray scattering analysis.[24] Similarly, the Fresnel contrast in Figs. 6(a) and 6(b) may result from the decomposition of volatile-rich fluorapatite and subsequent mass loss of volatile elements during the formation of the porous tracks. However, in zircon there are no fringes outside of the amorphous tracks, and the contrast in the tracks remains constant as the focus condition is changed [Fig. 6(c)]. This suggests that the inner potential difference between the tracks in zircon and the surrounding matrix is too small to show Fresnel contrast. The mass loss during the formation of an amorphous track is insignificant as compared to a porous track.

B. Formation of the porous tracks in fluorapatite

There has been considerable debate about the mechanism for the formation of fission tracks.[1,3] The thermal spike model treats the rapid deposition of energy into the lattice as a near-instantaneous heating event.[25,26] An alternative theory is the ion explosion model, by which the rapidly moving positively charged particle leaves a zone of positively ionized lattice atoms that are displaced from their original lattice sites as a result of Coulombic repulsion.[6,27] As an example, the lateral optical density profiles that are observed in tracks created by U or Fe ions in AgCl show a directly visible lack of central trace.[28] The authors suggest that the "hollow" track is caused by recombination effects and structural distortions due to "Coulombic repulsion."[28]

As the formation of porous tracks in LiF,[24] the formation of porous tracks in fluorapatite is the result of the deposition of highly ionizing energy that causes the radiolytic decomposition of fluorapatite accompanied by the loss of volatile elements. We performed *in situ* energy dispersive x-ray spectroscopy (EDS) analysis to qualitatively understand the compositional change in fluorapatite under the ionizing irradiation that causes track formation (Fig. 7). The electron beam was focused (~ 0.2 μm^2) in order to expedite the decomposition process (particle size ~ 500 nm and beam current ~ 5 A/cm^2). Under continuous electron-beam irradiations, the volatile elements can either escape to the vacuum in the TEM column, resulting in a loss of these elements in the EDS spectrum, or accumulate as bubbles in the bulk sample with CaO-rich rims forming gradually in the surrounding matrix.[29,30] The normalized loss of each major element in fluorapatite is plotted as a function of the time of the electron irradiation (Fig. 7). The normalized loss of F is the highest, followed by O and then P, which confirms that F is more readily sublimated than the other elements. The EDS analysis confirms that under electron-beam exposure there was a continuous release of "volatile" elements. Assuming similar material decomposition under ionizing particle irradiation, the porous fission tracks may retain some of the volatile elements from the matrix but this has not been confirmed.

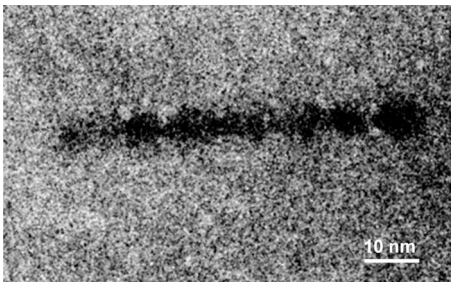

FIG. 8. HAADF Z-contrast STEM image. The darker contrast of the fission track in fluorapatite indicates a much lower total mass or thickness within the track core.

We note that the decomposition of fluoraptite during track formation may be different from that which occurs during electron-beam irradiation. In the case of electronic energy deposition by a fission fragment, track formation, and decomposition occurs over an extremely short time ($\sim 10^{-11}$ s) and thus is different from electron-beam-induced processes in many respects. In fluorapatite, the electronic energy deposition along the trajectory of fission fragments is of the order 10–18 keV/nm. This is much higher than the mean energy transfer of electrons (~ 0.8 eV/nm). However, the region exposed to the electron beam is significantly larger. By prolonged irradiation (up to 118 min), a sufficient dose was accumulated in order to decompose the target material. Since the decomposition process of fluorapatite during track formation is difficult to directly investigate experimentally, the EDS analysis of compositional change under electron exposure provides important qualitative information. For example, the volatile elements are more readily released, which is true in both cases despite of the differences mentioned above.

Information on the mass difference between the track core and the surrounding matrix were provided by high angle annular dark field (HAADF) scanning transmission electron microscopy (STEM) Z-contrast images (Fig. 8). The dark contrast is a clear indication of significant loss of matter along the track trajectory. This observation is consistent with the EDS results of the mass loss under electron irradiation. Irradiation-induced decomposition has been seen in many target materials.[29,31,32] However, the decomposition of volatile-rich materials is likely irreversible due to the loss of the volatile elements. The extent to which the volatile elements are released depends on the temperature and the interaction of the track with the surrounding matrix. The intense

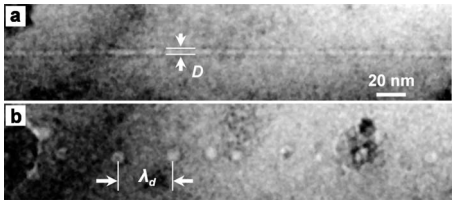

FIG. 9. Thermally induced Rayleigh instability. Fragmentation into spherical segments after *ex situ* heating (700 °C, 2 h, 1 atm Ar atmosphere) of a fission track in fluorapatite. Bright field image of single track (a) before and (b) after annealing (the same track is identified by means of markers made on the TEM copper grid). D, initial track diameter, and λ_d, spacing between droplets.

pressure around the track zone may assist in the escape of sublimated volatile elements from the track core[17] because the fission track (16–21 μm long and ~5 nm wide) may well pass through planar defects, such as fractures or even another fission track.[3] Alternatively, the porous track may be filled with gas via interactions with the solid at elevated temperatures[33] or even with the external atmosphere. At any rate, a fission fragment or swift heavy ion track in apatite is a highly porous channel that may be filled with a gas but the track does not contain an amorphous solid.

C. Thermal annealing of tracks

Ex situ thermal annealing experiments were conducted in order to observe the morphological change in the same fission track in fluorapatite before and after external furnace heating (Fig. 9). After taking images of fresh fission tracks, the grid with crushed samples was removed from the TEM and sealed in a glass tube filled with 1 atm Ar for furnace annealing. After the thermal treatment, the grid was inserted into TEM again to find the same fission tracks. A comparison of the morphologies of the same track shows a periodic segmentation into separate droplets after 2 h at 700 °C (Fig. 9). The self-organized segmentation of a highly porous fission track during annealing is driven by Rayleigh instability.[34–36] Similar segmentation of cylindrical voids (or pore channels) into separate droplets at elevated temperatures has been reported in alumina[36] and Ca-doped sapphire.[34] The driving force for the segmentation is the strong tendency toward lowering the total surface area due to the high diffusivity and the high surface tension of the pore channel.[34,35] In addition, the observations of the same tracks enable us to compare the volume change in tracks before and after furnace heating. The total volume of the remaining track in apatite shrinks significantly (Fig. 9). According to the void-growth/shrinkage law,[33] the thermal emission of vacancies from voids to surrounding solid can be neglected at low temperatures due to the low equilibrium vacancy concentration in the solid. Whereas, at high temperatures, the voids tend to evaporate rather than grow because of the rapid increase in the vacancy diffusion coefficient and the equilibrium vacancy concentration in the surrounding matrix, thus making thermal emission of vacancies from voids more favorable.[33]

There has been no study of *in situ* thermal evolution of the track microstructure despite a limited number of TEM investigations of latent track annealing.[37–39] No attention has been paid to the influence of different internal structures on the annealing behavior. We studied the morphological change in porous tracks in apatite *in situ* at 700 °C as a function of annealing time [Figs. 10(a)–10(d)]. Between the recording of TEM images, the electron beam was moved away to avoid electron-beam-induced changes. Within the first minute, the track becomes irregular with segments of smaller and larger radius but without much periodicity in the intervals [Fig. 9(b)]. After an annealing time in excess of 53 min, the fission track segments into random lengths along the ion trajectory [Figs. 10(c) and 10(d)]. According to Rayleigh instability, the rate of decay is very sensitive to the track radius; therefore, any deviation from a cylindrical shape along the track may cause a segmentation of tracks that lack of periodicity (Fig. 10). The track segmentation and the Brownian motion of track segments can be ascribed to the high mobility of atoms at the surface within the highly porous track structure.[33] This is in clear contrast to the annealing behavior of amorphous tracks in zircon, which gradually shrink and eventually disappear at 830 °C after 90 min due to defect elimination (Fig. 11). No track segmentation or Brownian motion of track segments in zircon was observed. This is because the surface tension and the diffusivity of atoms on the surface of amorphous tracks are too low for the track segmentation into separate droplets. The different annealing behaviors of the porous tracks in apatite and the amorphous tracks in zircon are consistent with their significant differences in internal structure.

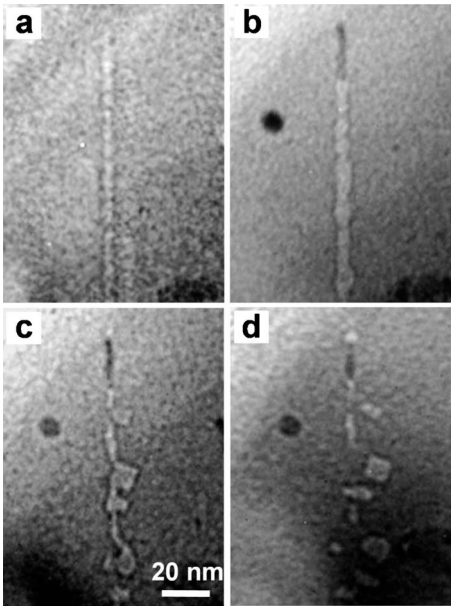

FIG. 10. *In situ* thermal annealing of fission tracks in fluorapatite. (a) Before heating and (b) after 1, (c) 53, and (d) 130 min heated at 700 °C, a fission track gradually segments into shorter lengths.

The mean lengths of etched track parallel to the c-axis (or [0001]) of fluorapatite are always larger than those perpendicular to the c-axis in all cases. This is known as the crystallographic effect.[40] The mechanism involved in the crystal-

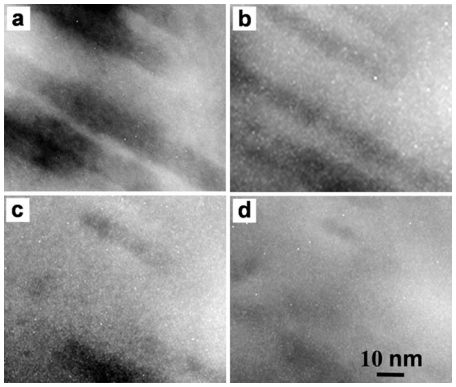

FIG. 11. *In situ* thermal annealing of tracks in zircon caused by 2.2 GeV Au ions. (a) Before heating, and (b) after 10, (c) 53, and (d) 90 min heated at 830 °C, the amorphous tracks began fading and eventually disappeared due to defect elimination.

lographic effect remains unknown because there have been no experiments to directly show the dynamic process of track annealing. We observed this effect in the "unetched" tracks in fluorapatite with thermal treatment at 700 °C by *in situ* TEM (Fig. 12). The tracks perpendicular to the *c*-axis segment faster than those parallel to the *c*-axis because the track segments move along this axis. Finally, this results in the formation of several parallel segments along the *c*-axis, which rotate almost 90° from the original ion trajectory. The preferred diffusion path of atoms along the *c*-axis accounts for the preferential motion of track segments.[1,33] Therefore, the slower segmentation of porous tracks parallel to the *c*-axis causes the longer lengths of etched tracks along this axis. The preferential motion of track segments in apatite can also be ascribed to the higher surface tension and the higher diffusivity of atoms on the surface of the highly porous tracks as compared to those of amorphous tracks. The random motion of atoms on the inside surface of bubbles (or voids) results in Brownian motion of the bubbles at elevated temperatures.[33] If the atoms move along a preferential direction, the bubbles preferentially move in this direction.[33] The similarities in the segmentation and motion between fission tracks and bubbles further confirm the tracks in fluorapatite are voids or bubbles.

IV. CONCLUSION

We have clearly shown that track annealing in fluorapatite is a complex process with several underlying mechanisms. The porous structure of latent tracks is critical to developing a physical description for fission track fading in fluorapatite at elevated temperatures. The damage recovery in a porous track is mainly driven by Rayleigh instability and Brownian or preferential motion of highly porous segments, in addition to the shrinkage of porous tracks by thermal emission of vacancies to the surrounding solid. Based on microscale studies on chemically etched tracks, it has generally been assumed that fission tracks in apatite completely anneal and disappear at temperatures of 360 °C within 60 min.[7,8] This is not the case, as demonstrated by high-resolution electron microscopy observations of track annealing. Remnants of the tracks, in the form of isolated segments, are still present at 700 °C even after times in excess of 130 min. In comparison, direct observation shows that the amorphous tracks in zircon disappear at 830 °C after 90 min, which agrees well with the etched tracks fading to completion at 800 °C after 60 min.[10] This comparison suggests that the discontinuities in porous tracks due to thermal treatment impede the etching agent from reaching the other sections of tracks for continued etching, thereby significantly reducing the effectiveness of chemical etching.[4,13] In contrast, the amorphous tracks in zircon do not segment, and fade in a continuous way at elevated temperatures. Etched tracks of zircon and apatite are both widely used for fission track dating but this difference in the annealing behavior of latent tracks between these two important minerals has not been previously addressed.

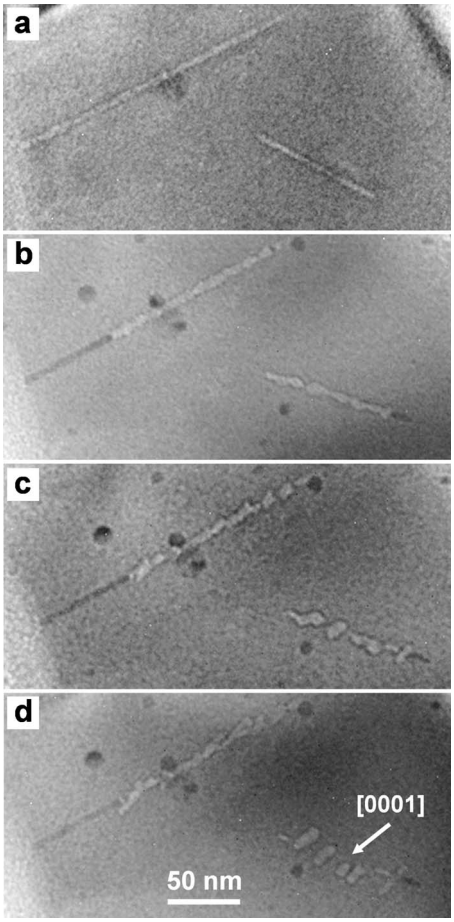

FIG. 12. Crystallographic effect. *In situ* TEM images showing the preferential motion of fission track segments along [0001] of fluorapatite and the slower fragmentation of tracks along this direction during thermal treatment. (a) Before annealing, and (b) after 1, (c) 17, and (d) 60 min heated at 700 °C.

ACKNOWLEDGMENTS

The funding for this study was provided by the Office of Basic Energy Sciences of the U.S. DOE (Grant No. DE-FG02-97ER45656). M.L. acknowledges support from the German Research Foundation (DFG).

*lmwang@umich.edu
†rodewing@umich.edu

[1] A. J. W. Gleadow, D. X. Belton, B. P. Kohn, and R. W. Brown, Rev. Mineral. Geochem. **48**, 579 (2002).
[2] J. A. L. Rabone, A. Carter, A. J. Hurford, and N. H. de Leeuw, Phys. Chem. Miner. **35**, 583 (2008).
[3] T. Tagami and P. B. O'Sullivan, Rev. Mineral. Geochem. **58**, 19 (2005).
[4] F. Villa, M. Grivet, M. Rebetez, C. Dubois, A. Chambaudet, A. Chevarier, P. Martin, F. Brossard, G. Blondiaux, T. Sauvage, and M. Toulemonde, Radiat. Meas. **31**, 65 (1999).
[5] M. Lang, J. Lian, F. Zhang, B. W. H. Hendriks, C. Trautmann, R. Neumann, and R. C. Ewing, Earth Planet. Sci. Lett. **274**, 355 (2008).
[6] R. L. Fleischer, P. B. Price, and R. M. Walker, *Nuclear Tracks in Solids* (University of California Press, Berkeley, 1975), p. 31.
[7] K. D. Crowley, M. Cameron, and R. L. Schaefer, Geochim. Cosmochim. Acta **55**, 1449 (1991).
[8] P. F. Green, I. R. Duddy, A. J. W. Gleadow, P. R. Tingate, and G. M. Laslett, Chem. Geol. **59**, 237 (1986).
[9] W. D. Carlson, Am. Mineral. **75**, 1120 (1990).
[10] R. Yamada, T. Tagami, S. Nishimura, and H. Ito, Chem. Geol. **122**, 249 (1995).
[11] K. D. Crowley, Am. Mineral. **78**, 210 (1993).
[12] P. F. Green, G. M. Laslett, and I. R. Duddy, Am. Mineral. **78**, 441 (1993).
[13] A. Meftah, F. Brisard, J. M. Costantini, M. Hage-Ali, J. P. Stoquert, F. Studer, and M. Toulemonde, Phys. Rev. B **48**, 920 (1993).
[14] J. Vetter, R. Scholz, D. Dobrev, and L. Nistor, Nucl. Instrum. Methods Phys. Res. B **141**, 747 (1998).
[15] A. Adla, H. Fuess, and C. Trautmann, J. Polym. Sci. Pol. Phys. **41**, 2892 (2003).
[16] J. Jensen, A. Dunlop, and S. Della-Negra, Nucl. Instrum. Methods Phys. Res. B **141**, 753 (1998).
[17] G. Jaskierowicz, A. Dunlop, and R. Jonckheere, Nucl. Instrum. Methods Phys. Res. B **222**, 213 (2004).
[18] K. Sun, L. M. Wang, and R. C. Ewing, Nucl. Instrum. Methods Phys. Res. B **266**, 3133 (2008).
[19] S. Bysakh, M. Shimojo, K. Mitsuishi, and K. Furuya, J. Vac. Sci. Technol. B **22**, 2620 (2004).
[20] D. B. William and C. B. Carter, *Transmission Electron Microscopy* (Plenum Press, New York and London, 1996), pp. 82–450.
[21] T. Malis, S. C. Cheng, and R. F. Egerton, J. Electron Microsc. Tech. **8**, 193 (1988).
[22] Z. Zhang and D. Su, Ultramicroscopy **109**, 766 (2009).
[23] E. Borowiak-Palen, E. Mendoza, A. Bachmatiuk, M. H. Rummeli, T. Gemming, J. Nogues, V. Skumryev, R. J. Kalenczuk, T. Pichler, and S. R. P. Silva, Chem. Phys. Lett. **421**, 129 (2006).
[24] S. A. Saleh and Y. Eyal, Nucl. Instrum. Methods Phys. Res. B **230**, 246 (2005).
[25] A. Meftah, F. Brisard, J. M. Costantini, E. Dooryhee, M. Hage-Ali, M. Hervieu, J. P. Stoquert, F. Studer, and M. Toulemonde, Phys. Rev. B **49**, 12457 (1994).
[26] L. T. Chadderton, Radiat. Meas. **36**, 13 (2003).
[27] R. L. Fleischer, P. B. Price, and R. M. Walker, J. Appl. Phys. **36**, 3645 (1965).
[28] E. Schopper, B. Baican, H.-G. Baumgardt, and K. O. Groeneveld, Radiat. Meas. **25**, 79 (1995).
[29] A. Meldrum, L. M. Wang, and R. C. Ewing, Am. Mineral. **82**, 858 (1997).
[30] M. Cameron, L. M. Wang, K. D. Crowley, and R. C. Ewing, in *Proceedings of the 50th Annual Meeting of the Microscopy Society of American*, edited by G. W. Bailey, J. Bentley, and J. A. Small (San Francisco Press, San Francisco, 1992), p. 378.
[31] L. P. Zenser, R. Gruehn, and B. H. Liebscher, J. Solid State Chem. **157**, 30 (2001).
[32] A. Meldrum, S. J. Zinkle, L. A. Boatner, and R. C. Ewing, Nature (London) **395**, 56 (1998).
[33] D. R. Olander, *Fundamental Aspects of Nuclear Reactor Fuel Elements* (NTIS, US Dept. of Commerce, Springfield, VA, 1976), p. 236.
[34] A. M. Glaeser, Interface Sci. **9**, 65 (2001).
[35] F. A. Nichols and W. W. Mullins, Trans. Metall. Soc. AIME **233**, 1840 (1965).
[36] T. K. Gupta, J. Am. Ceram. Soc. **61**, 191 (1978).
[37] P. B. Price and R. M. Walker, J. Appl. Phys. **33**, 2625 (1962).
[38] T. A. Paul and P. G. Fitzgerald, Am. Mineral. **77**, 336 (1992).
[39] T. A. Paul, Nucl. Tracks Radiat. Meas. **21**, 507 (1993).
[40] R. A. Donelick, Am. Mineral. **76**, 83 (1991).